Supporting Information

Tracking a Common Surface-Bound Intermediate during CO_2-to-Fuels Catalysis

Anna Wuttig,† Can Liu,‡ Qiling Peng,‡ Momo Yaguchi,‡§ Christopher H. Hendon,† Kenta Motobayashi,‡ Shen Ye,‡ Masatoshi Osawa,‡ and Yogesh Surendranath†*

†Department of Chemistry, Massachusetts Institute of Technology, Cambridge, MA 02139, United States

‡ Institute for Catalysis, Hokkaido University, Sapporo 001-0021, Japan

§ Graduate School of Environmental Science, Hokkaido University, Sapporo 060-0810, Japan

yogi@mit.edu

Index *Page*

Experimental Methods

Materials. Na_2CO_3 (≥ 99.9999 % TraceSELECT®) and 2-2' bipyridine (≥ 99 %) were purchased from Sigma Aldrich. CO_2 (Ultra High Purity) was purchased from SI Science or Airgas. Ar (Ultra High Purity), CO (Ultra High Purity), and ^{13}CO (99 %) were purchased from SI Science. $CuSO_4 \cdot 5H_2O$ was purchased from Wako Pure Chemicals (99.9 %) or Strem chemicals (99.999 %). HCHO (36-38% assay, stabilized with 5-10% methanol) was purchased from Wako Pure Chemicals or Sigma Aldrich. NaOH (Cica-Reagent, 97%) and NaOH (Semiconductor grade, 99%) were purchased from Kanto Chemical and Sigma Aldrich, respectively. HF (49.5-50% aqueous solution) was purchased from Kanto Chemical or Sigma Aldrich. Na_2EDTA was purchased from Dojindo Dotite (99.5%) or Sigma Aldrich (ACS Reagent). NH_4F (40% aqueous solution) was purchased from Morimoto Chemicals or Sigma Aldrich. All chemicals were used as received without further purification. Millipore Type 1 water (18.2 MΩ) was used throughout the study. In all cases, electrolytes were purified using regenerated Chelex100 (Bio-Rad), according to manufacturer's protocol with slight modifications.[1] Bicarbonate electrolytes (0.1 M $NaHCO_3$) were prepared by sparging CO_2 through a purified Na_2CO_3 solution with a concentration half that of the desired final bicarbonate concentration.

Preparation of Cu Films for Surface Enhanced Infrared Spectroscopy Analyses. A thin Cu film (~80-nm thick) was chemically deposited on the reflecting plane of a hemicylindrical Si prism (Pier Optics, Japan) by an electroless plating technique. For AFM and XPS data (Figures 1, S1, S2, and S3), Si wafers (Global Top Chemical, Japan) were utilized because the hemicylinder does not fit into the AFM and XPS chambers. The synthesis of Cu on the Si prism and wafer differed only by the time duration of the cleaning of the Si substrate. The Si wafers were polished using 1 μm alumina for 3 minutes while the Si prism was polished using 1 μm alumina for 10 minutes. This procedure rendered the Si surfaces hydrophobic as judged by the tendency of water to bead rather than wet the surface. The Si surfaces were then rubbed with a wet Kimwipe under flowing water for 3-10 minutes until the surface became hydrophilic, as judged by uniform wetting of water across the surface. Subsequently, the Si surfaces were sonicated in MilliQ water, then acetone, then MilliQ water for 10, 5, and 5 minutes respectively. Si surfaces were then immersed in 40% NH_4F for ~30 seconds until the surface became hydrophobic. This procedure yielded the etched Si surface which was characterized by AFM (Figure S1a and b). The etched Si surfaces were then immersed for 90 s in 0.5% HF containing 750 μM $CuSO_4$, generating a hydrophilic surface containing a Cu seed layer as characterized by AFM (Figure S1c and d). Following Cu seed deposition, the surfaces were immersed for 210 s in a ~54 °C, pH 12, deposition bath containing 0.25 M HCHO, 0.02 M $CuSO_4$, 20 mM Na_2EDTA, and 0.3 mM 2,2-bipyridine to yield a Cu mirror surface as characterized by AFM (Figure S1e and f). $CuSO_4$, HCHO, and Na_2EDTA/2,2-bipyridine/pH 12 solutions were prepared in three separate vials. The solutions were mixed to the final concentration listed above by adding the Na_2EDTA/2,2-bipyridine/pH 12 solution dropwise to a mixture of $CuSO_4$ and HCHO and heated to temperature ~10 min before deposition. The resulting Cu film displayed a resistance of 7 to 27 Ω as measured across the diagonal using an ohmmeter. Between each of the preceding steps, Si etching, seed deposition, and film growth, the substrates were rinsed gently under a constant stream of MilliQ water. Following preparation, films were immediately assembled into the electrochemical cell. Bicarbonate electrolyte was carefully added to the electrochemical cell prior to the initiation of SEIRAS measurements. In all cases, the films were exposed to the electrolyte used for the experiment within 1 hr of film preparation. Once enclosed in the cell, the films were cycled between open circuit (–0.13 V vs Ag/AgCl) and –0.70 V vs Ag/AgCl three times to clean the surface and reduce adventitious surface oxides. The data reported in Figure 1b were smoothed using a Savitzy-Golay 2nd order polynomial to remove noise caused by CO_2 bubbling during the measurement. Following this initial CV cycling, the Cu films were polarized between –0.35 V and –0.45 V vs Ag/AgCl between each measurement to prevent the reformation of surface oxides. We observed that, following polarization, exposing the electrode to potentials positive of this range would induce delamination of the film. Therefore, for each pH environment examined, the cell had to be disassembled to introduce new electrolyte and thus a new SEIRAS-active film was employed in the subsequence measurement. The data reported in Figures 2a, S5, S6, and S7 made use of the same SEIRAS-active Cu film electrode. A separate film electrode, prepared in an identical fashion, was used to collect the data shown in Figures 2b, 2c, and S8. A separate film electrode, prepared in an identical fashion, was used to collect the data shown in Figures 3, 4 (pH 6.9), S4, and S9. A separate film electrode, prepared

in an identical fashion, was used to collect the data shown in Figures 4 (pH 7.8), S11a, and S11c. A separate film electrode, prepared in an identical fashion, was used to collect the data shown in Figures 4 (pH 10.1), 5, S11b, S11d, and S12.

Atomic Force Microscopy. The morphology of the surface was imaged after each step of the synthesis by atomic force microscopy, AFM, (Asylum Research Olympus IX71) in tapping mode using a silicon cantilever (OMCL-AC240TS-C2, radius of 7 nm, spring constant of 2 N/m, resonance frequency of 70 kHz, Olympus). AFM studies were conducted on Si wafers rather than Si prisms.

X-Ray Photoelectron Spectroscopy. X-ray photoelectron spectra were collected on as-synthesized Cu-coated Si surfaces. The surface was rinsed thoroughly with MilliQ water and dried under ambient conditions before being loaded into the ultra high vacuum chamber. XPS samples were prepared by adhering the electrodes to the sample stage with conducting carbon tape. The X-ray photoelectron spectra were collected using a JPC-9010MC (JEOL) with a hemispherical energy analyzer and a monochromated X-ray source (Magnesium Kα, 1253.6 eV). Data were collected using a 6 mm, 100 W focused X-ray beam at a base pressure of 5×10^{-8} torr. Wide-scan survey data were collected with a pass energy of 50 eV and a step size of 1.0 eV. Narrow scans over peaks of interest were collected with a pass energy of 10 eV and a step size of 0.1 eV. The C 1s peak arising from adventitious hydrocarbons was assigned the energy value 284.0 eV and used as an internal binding energy reference.

Electrochemical Methods. All electrochemical experiments were conducted using either a EG&G PAR model 263A or Gamry REF 600 potentiostat, a leakless Ag/AgCl electrode (eDAQ), and a high surface area Pt-mesh counter electrode (Alfa Aesar, 99.997 %). Ag/AgCl reference electrodes were stored in Millipore water between measurements and were periodically checked relative to pristine reference electrodes to ensure against potential drift. All experiments were performed at ambient temperature, 20 ± 2 ºC. Electrode potentials were converted to the reversible hydrogen electrode (RHE) scale or the standard hydrogen electrode (SHE) scale using $E_{RHE} = E_{Ag/AgCl} + 0.197\ V + 0.059(pH)$ or $E_{SHE} = E_{Ag/AgCl} + 0.197\ V$. Potentials were corrected for uncompensated Ohmic loss (iR_u) in situ via positive feedback. R_u was measured prior to each experiment using the R_u test function in the Model 270/250 Research Electrochemistry Software 4.11 or the Gamry Framework Software. All current density values are reported relative to the geometric surface area of the working electrode. The three-compartment spectroelectrochemical cell held ~35 mL of electrolyte. The details of ATR-SEIRAS cell configuration have been described elsewhere.[2–7] Prior to assembly, the cell was cleaned for at least 1 hour in a concentrated H_2SO_4:HNO_3 mixture, rinsed with Millipore water thoroughly, sonicated for at least 1 hour in Millipore water, and stored in fresh Millipore water prior to all experiments. A water tight seal was formed between the Cu-film coated Si prism and the electrochemical cell using a Kalrez vacuum O-ring (i.d.= 15 mm). The Pt mesh was housed in a counter compartment separated from the working chamber by a porous glass frit. The reference electrode was separated from the working electrode via a Luggin capillary.

Double Layer Capacitance Measurements. Roughness factors of the synthesized Cu films on Si substrates were determined via double layer capacitance measurements. The samples were cycled in the double layer charging region from −0.60 V to −0.70 V vs Ag/AgCl at a scan rate of 20, 40, 60, 80, and 100 mV s^{-1} in the CO_2 or Ar-saturated 0.1 M bicarbonate electrolyte used for subsequent SEIRAS studies (pH 6.8, 6.9, 7.8, or 10.1) to obtain the representative data shown in Figure S4. The slopes of the double layer charging current vs the scan rate were divided by two to determine the double layer capacitance, which was then divided by the reference double layer capacitance measured for a polished Cu surface[8] to determine a roughness factor of 10.5 ± 0.4. The roughness factor was found to be invariant over the course of a SEIRAS measurement (Figure S4).

Surface-Enhanced Infrared Absorption Spectroscopy (SEIRAS). SEIRA spectra were recorded in the Kretschmann attenuated total reflection (ATR) configuration using a Bio-Rad FTS-60A/896 FTIR spectrometer equipped with a HgCdTe (MCT) detector and a homemade single-reflection accessory (incident angle of 60°). The spectrometer was operated in kinetic mode (40 kHz). Spectra were sequentially acquired with a spectral resolution of 4 cm^{-1} at 4.875 s intervals for cyclic voltammetry measurements (Figures 2a, 3, 4, 5, S5, S9, S11, S12) or 0.101 s

interval (Figure 2b, 2c, and S8) for chronoamperometry measurements. A single beam spectrum collected at the starting potential, as indicated in the description for each experiment described below, was used as the reference spectrum. All ATR-SEIRA spectra are reported in absorbance units defined as $A=-\log(I/I_0)$, where I and I_0 denote the light intensity for the sample and reference single-beam spectra, respectively.

Potential-dependence of Electrogenerated CO. Prior to each experiment, the 0.1 M $NaHCO_3$ electrolyte was sparged with 1.0 atm of CO_2 at 40 sccm for 15 min (Figures 2a, S5, S6, and S7). The background was acquired at –0.35 V vs Ag/AgCl (0.25 V vs RHE). During all experiments, the electrolyte was sparged continuously with 1.0 atm of CO_2 at 20 sccm. Cyclic voltammograms were recorded at 2 mV s^{-1}, and spectra were simultaneously acquired.

Faradaic Efficiencies of SEIRAS-active Cu films. Cu films on Si substrates (University Wafer ID 444 Si (100) P/B) were prepared in an identical fashion to that used in the spectroelectrochemical cell. These films were evaluated for CO_2 reduction catalysis using in-line gas chromatography (GC, SRI Instruments, Multi-Gas Analyzer #3) equipped with a thermal conductivity detector, methanizer, and flame ionization detector in series following Molsieve 13x and Hayesep D columns. The Cu on Si substrate was assembled into an electrode by connecting it to a Ti wire and cleaned via the same electrochemical treatment as applied to the surfaces examined by SEIRAS. The Cu films were polarized at –1.10, –1.30, –1.50, and –1.70 V vs Ag/AgCl (corresponding to –0.50, –0.70, –0.90, and –1.10 V vs RHE, respectively) in 1.0-atm CO_2-saturated 0.1 M $NaHCO_3$. The electrolyte was sparged continuously with CO_2 at 10 sccm during the experiments. Measurements were conducted in an airtight H-cell (25 mL catholyte and 20 mL anolyte) separated by an anion exchange membrane (AGC Selemion membrane). Prolonged electrolysis, at least 20 min at each potential, is necessary to ensure a steady-state equilibration between the produced gasses and the carrier stream and to allow for detection of higher order products via GC. Prior to each experiment, the uncompensated cell resistance was measured and typically ranged from 15 to 22 Ω. The partial current density (j_p) for each CO_2 reduction product, p, was calculated using the following relationship: j_p = [p]*flow rate*nFP/RT*1/area. [p] is the ppm value of the product measured via GC using an independent calibration standard gas mixture, n is the number of electrons transferred per equivalent of p, P is the pressure in the electrochemical cell headspace (1.1 atm), T is the temperature, and F is Faraday's constant. The partial current density for a given product is divided by the total current density, averaged over a 35 s span immediately prior to each GC run, to determine its partial Faradaic efficiency. These prolonged electrolysis conditions are far more aggressive than the potential sweep experiments used for spectroscopic runs, and we observed that under prolonged electrolysis at reducing potentials beyond –0.80 V vs RHE, the Cu films progressively delaminate from the Si surface. The data shown in Figure S10 are the average and standard deviation of three independently prepared samples. Although the data are convoluted by partial film delamination, we do observe that SEIRAS-active Cu films are capable of generating higher order products with an onset of methane production at –0.90 V vs RHE and ~20% methane at –1.1 V vs RHE.

Time-dependence of Electrogenerated CO. SEIRA spectra were collected every 0.191 s while the copper film was polarized at –0.45 V vs Ag/AgCl (0.15 V vs RHE) for 30 s and then immediately stepped to –1.40 V vs Ag/AgCl (–0.80 V vs RHE) for 330 s in 1.0-atm CO_2-sparged 0.1 M $NaHCO_3$ (Figure S8). The background trace was collected in advance at –0.45 V vs Ag/AgCl (0.15 V vs RHE). 1.0 atm of CO_2 was delivered to the electrolyte at 20 sccm for 1 hour prior to data collection and during the run. The broad band was integrated from 2120 and 1960 cm^{-1} and plotted as a function of time.

^{13}CO Exchange Study. Prior to all experiments, the 0.1 M $NaHCO_3$ electrolyte was sparged with 1.0 atm CO_2 at 40 sccm for 15 min (Figures 2b and c). The background was acquired at –0.45 V vs Ag/AgCl (0.15 V vs RHE). During all experiments, the electrolyte was sparged continuously with 1.0 atm of CO_2 at 20 sccm. The Cu foil was polarized at –0.45 V vs Ag/AgCl (0.15 V vs RHE) for 30s, after which it was polarized at –1.40 V vs Ag/AgCl (–0.80 V vs RHE) for 330s. Spectra were acquired simultaneously, and ^{13}CO was introduced at 20 sccm after a steady-state current at –1.40 V vs Ag/AgCl (–0.80 V vs RHE) was achieved.

CO Adsorption Profiles at a Single and Varying pH. Prior to all experiments, the bicarbonate electrolyte was sparged for 30 min at 20 sccm with either 0.75 atm CO_2 and 0.25 atm Ar to maintain a pH of 6.9, or 0.10 atm CO_2 and 0.90 atm Ar to maintain a pH of 7.8, or 1.0 atm Ar to maintain a pH of 10.1 (Figures 3, 4, 5, S9, S11, and S12). During all experiments, the electrolyte was sparged continuously with Ar/CO_2, CO/CO_2, Ar/CO_2/CO, or Ar/CO to maintain the desired partial pressure of CO. The CO partial pressure was controlled by changing the relative flow rates of CO to Ar while maintaining 0.75 atm CO_2 to collect data at pH 6.9 and 0.10 atm CO_2 to collect data at pH 7.8. The pH of the solution was measured using a pH probe after each experiment to confirm that the electrolyte pH has not drifted over the course of the SEIRAS measurement. The background spectra were acquired at –0.45 V vs Ag/AgCl for pH 6.9 (0.16 V vs RHE), –0.55 V vs Ag/AgCl for pH 7.8 (0.11 V vs RHE), and –0.85 V vs Ag/AgCl for pH 10.1 (–0.05 V vs RHE). Cyclic voltammograms were taken at 2 mV s^{-1}, and spectra were simultaneously acquired. The double layer capacitance was measured prior to and following every experimental run to ensure that the roughness factor did not change.

Calculation of Surface-Bound CHO and OCCO Vibrational Modes. First-principles total energy and electronic structure calculations were performed within the Kohn-Sham DFT construct. A delocalised plane-wave basis set with PAW scalar-relativistic frozen-core potentials were employed as implemented in the Vienna ab initio simulation package (VASP). A 500 eV plane-wave kinetic energy cutoff and a 4 x 4 x 1 k-grid were combined to provide total energy convergence to within 0.01 eV/atom. Beginning with the previously published structures for surface-bound OCCO and CHO on Cu(100),[9] shown in Figure S13, all unit cell vectors and internal atomic positions were relaxed to their equilibrium values using the PBEsol functional.[10] Vibrational frequencies were then computed using finite displacements, where only the organic-bound copper and the surface-bound organics were free to vibrate in three dimensions. Calculated vibrational modes for surface-bound OCCO and CHO intermediates are listed in Table S1. As a reference for spectroscopic studies reported in this work, vibrational modes for surface-bound CO were also computed in the same DFT construct. For Cu(111), Cu(110), and Cu(100) surfaces, the stretching frequency for linearly bonded CO at 6%, 13%, and 13% coverage, respectively, were calculated to be 2032, 2049, and 2039 cm^{-1}, respectively. These computed surface-bound CO stretching frequencies are well within the range we observe spectroscopically, 2104 and 1970 cm^{-1}.

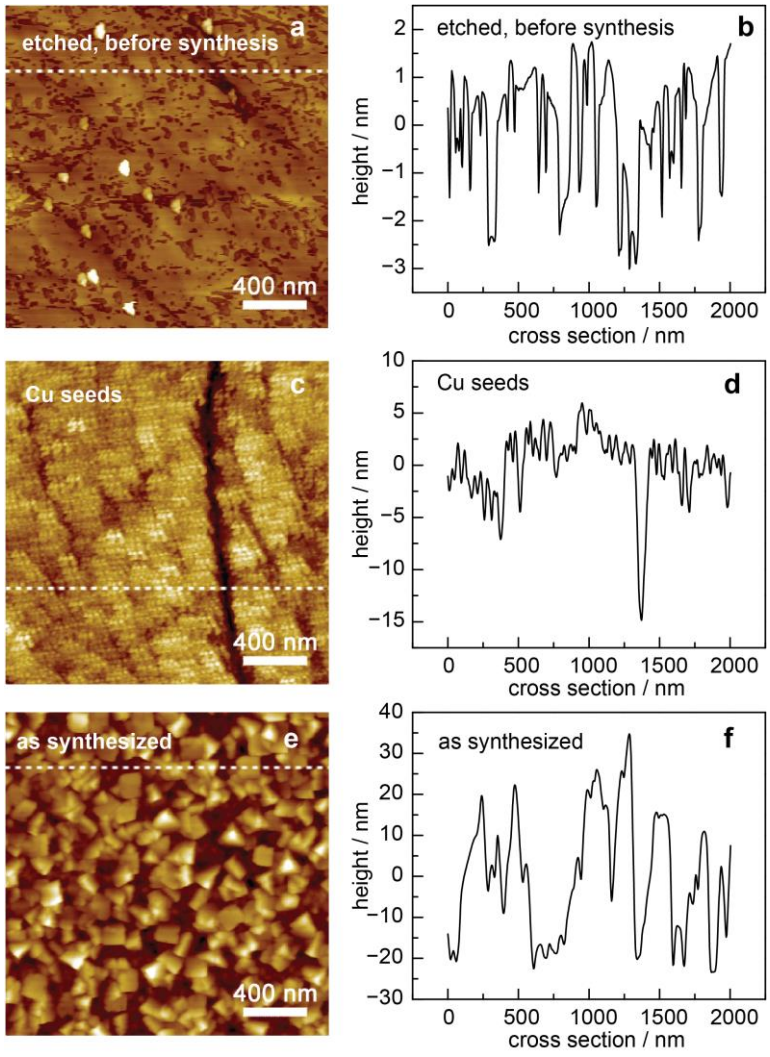

Figure S1. Atomic force microscopy (AFM) images of Si substrates along the synthetic sequence used to prepare SEIRAS-active Cu films used in this study. AFM image (**a**) and height profile along the dotted line (**b**) of an etched Si surface. AFM image (**c**) and height profile along the dotted line (**d**) of an etched Si surface following Cu seed growth in 0.5 % HF and 750 μM $CuSO_4$. AFM image (**e**) and height profile along the dotted line (**f**) of a Cu on Si film prepared from a ~54 °C, pH 12, deposition bath containing 0.25 M HCHO, 0.02 M $CuSO_4$, 20 mM Na_2EDTA, and 0.3 mM 2,2-bipyridine.

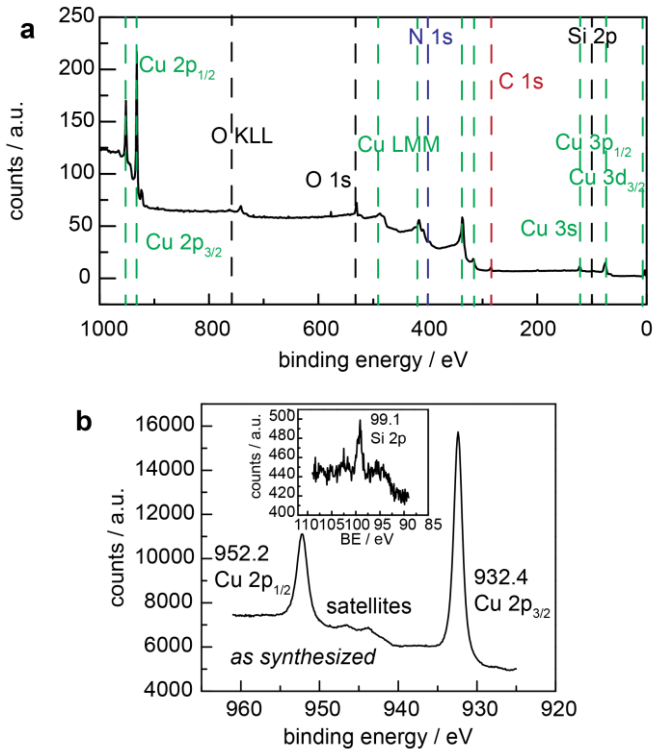

Figure S2. XPS spectra of an as-prepared Cu thin film electrode on a Si surface. Survey scan (**a**) and high-resolution spectrum of the Cu 2p (**b**) and Si 2p (**b, inset**) regions.

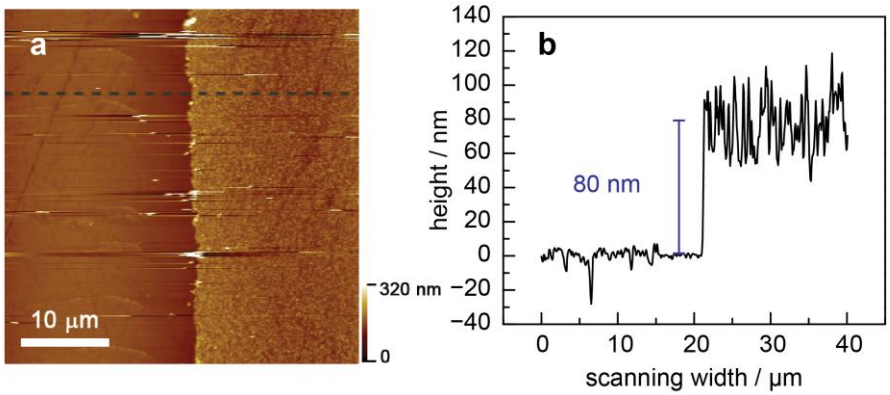

Figure S3. (**a**) Atomic force microscopy image and (**b**) corresponding height profile of a Cu thin film on a Si substrate that has been scratched to reveal the Si underlayer. The large height step (average height = 80 nm) corresponds to the edge of the substrate-exposed region.

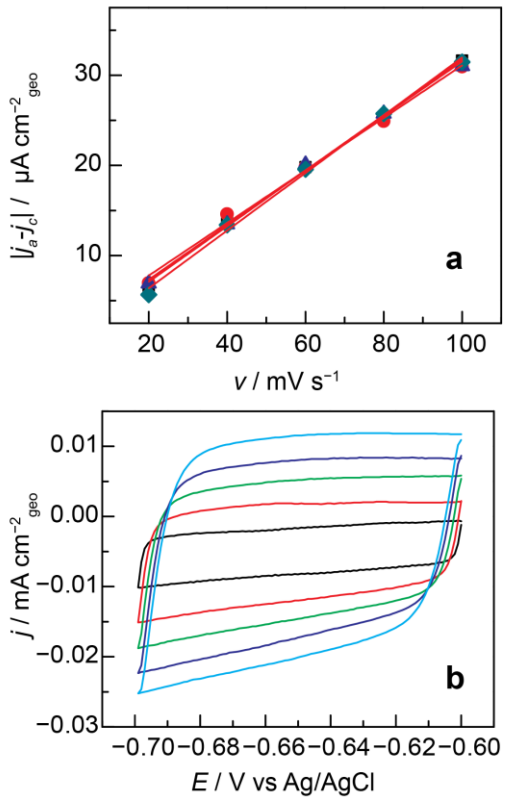

Figure S4. Roughness factor measurements. (**a**) Double layer charging current vs scan rate for a Cu thin film on a Si substrate recorded at –0.05 V vs RHE. Black squares correspond to data recorded before a SEIRAS run, whereas red circles, blue triangles, and cyan diamonds correspond to data recorded after one, two, and three ~30 min SEIRAS measurements, respectively. The slopes of the double layer charging current vs the scan rate were divided by two to determine the double layer capacitance, which was then divided by the reference double layer capacitance measured for a polished Cu surface[8] to determine a roughness factor of 10.5 ± 0.4. (**b**) Representative double layer capacitance measurements recorded at 20 (black), 40 (red), 60 (green), 80 (dark blue), and 100 (light blue) mV s^{-1} scan rate.

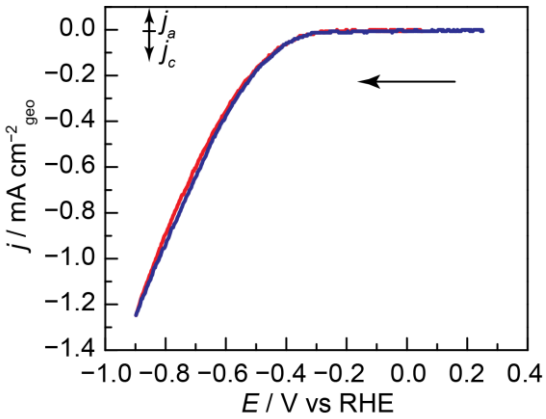

Figure S5. Representative cyclic voltammograms (CVs) collected during simultaneous SEIRA spectra acquisition shown in Figure 2a. CVs were recorded at 2 mV s^{-1} in 1.0-atm CO_2-saturated 0.1 M $NaHCO_3$, pH 6.8. The forward and reverse-going traces are shown in blue and red, respectively.

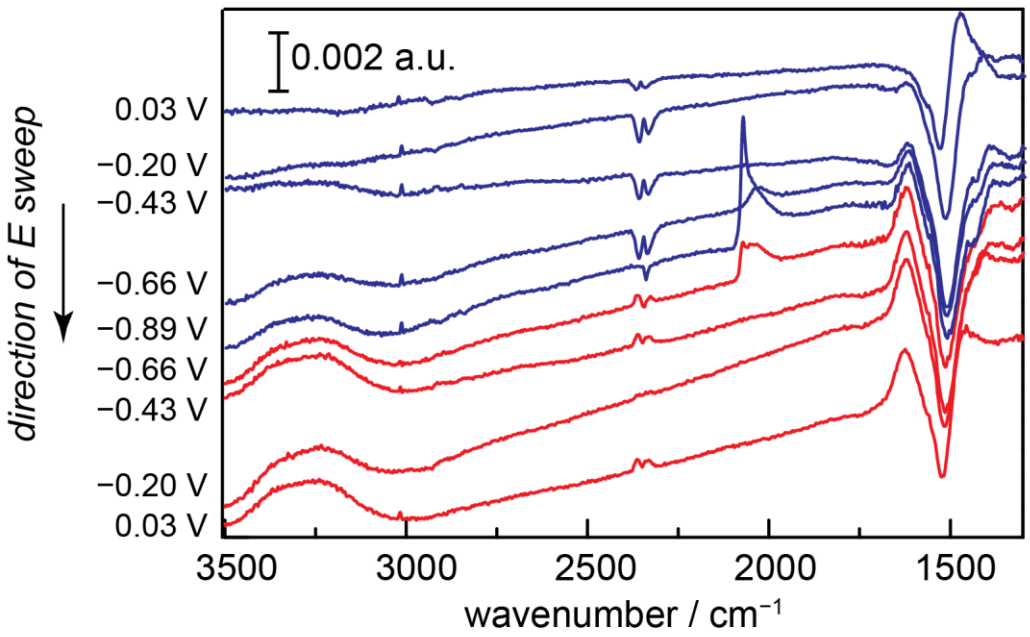

Figure S6. SEIRA spectra recorded during the forward-going (blue) and reverse-going (red) scan plotted over an expanded spectral window relative to the data shown in Figure 2a. Spectra were collected in 1.0 atm CO_2-saturated 0.1 M $NaHCO_3$, pH 6.8. The peaks spanning 2300 to 2380 cm^{-1} correspond to dissolved CO_2 in the electrolyte.

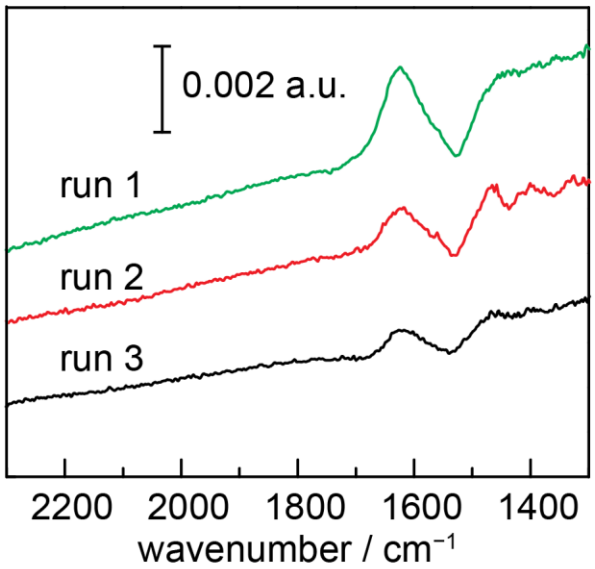

Figure S7. Final SEIRA spectra recorded at 0.25 V vs RHE in 1.0-atm CO_2-saturated 0.1 M $NaHCO_3$ over sequential runs. Comparison of first run (green), second run (red), and third run (black), show that the carbonate and water peak intensities decrease over the course of multiple runs.

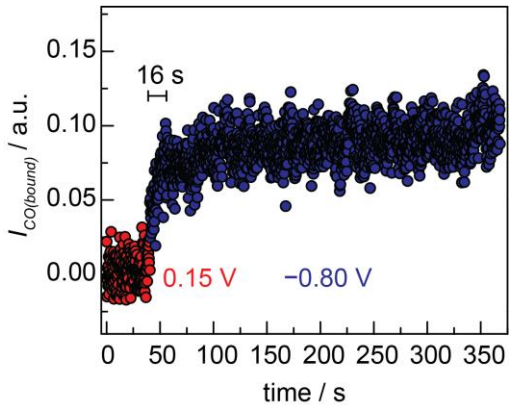

Figure S8. Time dependence of the evolution of the integrated band intensity corresponding to electrogenerated CO on a Cu surface recorded in 1.0-atm CO_2-saturated 0.1 M $NaHCO_3$. The electrode was polarized at 0.15 V for 30 s, then stepped to –0.80 V for 330 s.

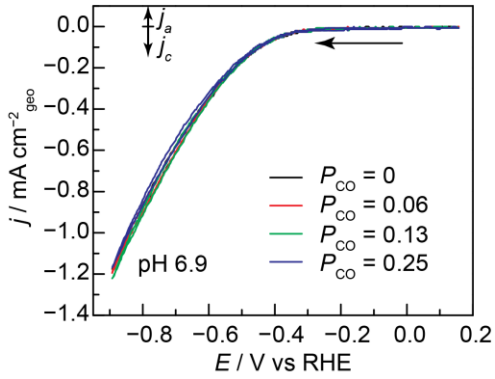

Figure S9. Cyclic voltammograms (CVs) recorded at pH 6.9 during the collection of CO adsorption profiles shown in Figure 3. CVs were collected at 2 mV s^{-1} scan rate in 0.75-atm CO_2-saturated 0.1 M $NaHCO_3$, pH 6.9, with P_{CO} = 0.00 atm (black), 0.06 atm (red), 0.13 atm (green), and 0.25 atm (blue). Argon was used as the balance gas in all cases.

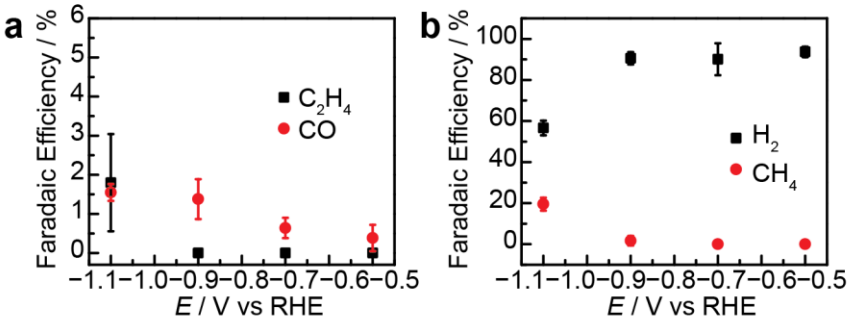

Figure S10. Faradaic efficiencies for C_2H_4 (black, **a**), CO (red, **a**), H_2 (black, **b**), and CH_4 (red, **b**) as a function of potential during controlled-potential electrolyses in 1.0-atm CO_2-saturated 0.1 M $NaHCO_3$ electrolyte on SEIRAS-active Cu films prepared on Si substrates. At reducing potentials beyond –0.80 V vs RHE, the Cu films progressively delaminate from the Si surface. The data shown are the average and standard deviation of three independently prepared samples and are convoluted by partial film delamination.

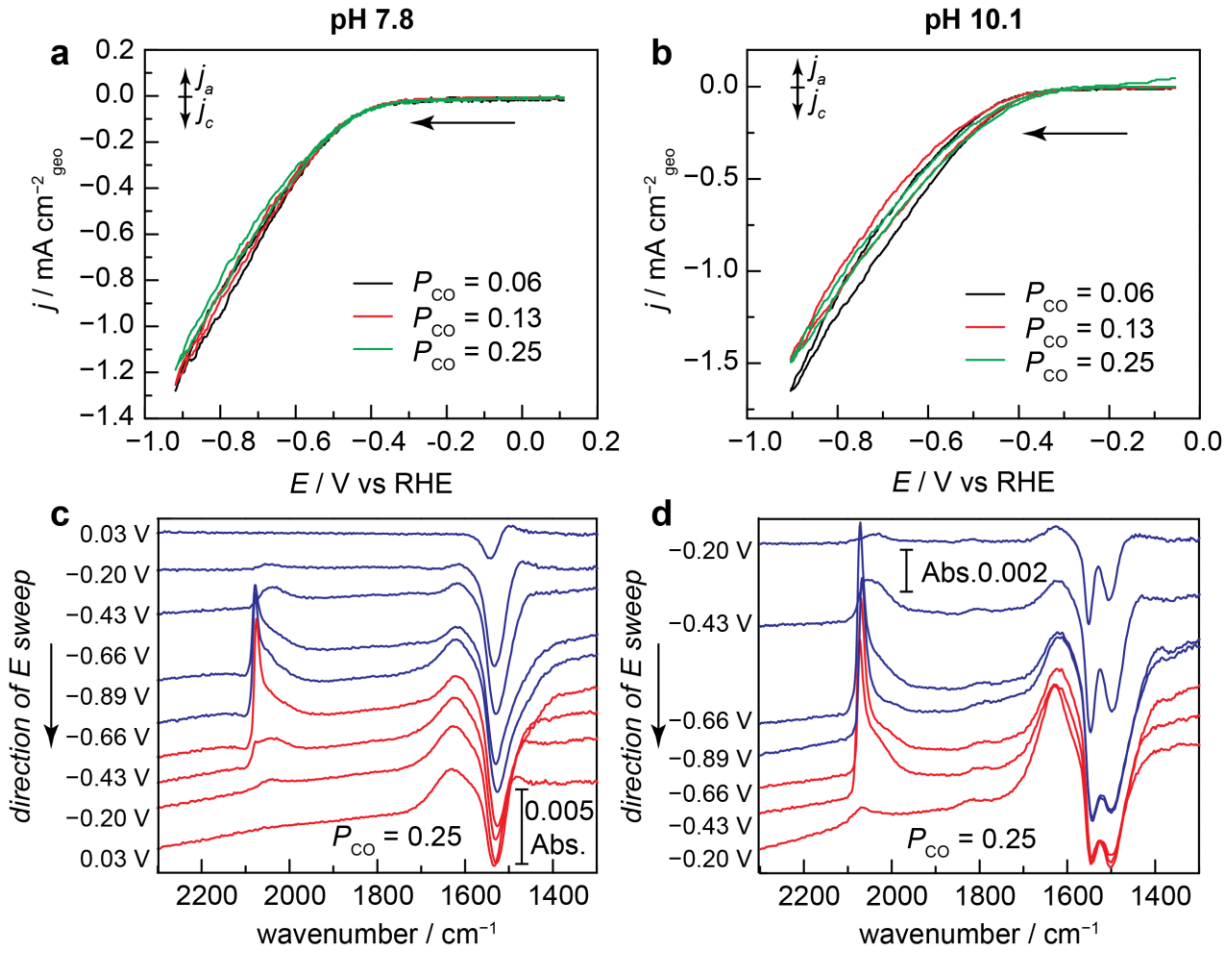

Figure S11. CVs and SEIRA spectra collected at elevated pH. (**a**) CVs recorded at 2 mV s^{-1} in 0.1-atm CO_2-saturated 0.1 M $NaHCO_3$, pH 7.8, with P_{CO} = 0.06 atm (black), 0.13 atm (red), and 0.25 atm (green). (**b**) CVs recorded at 2 mV s^{-1} in 0.75-atm Ar-saturated 0.1 M carbonate buffer, pH 10.1, with P_{CO} = 0.06 atm (black), 0.13 atm (red), and 0.25 atm (green). (**c**) SEIRA spectra collected during the CV scan in the presence of 0.25 atm P_{CO} at pH 7.8 (green trace in Figure S11a). (**d**) SEIRA spectra collected during the CV scan in the presence of 0.25 atm P_{CO} at pH 10.1 (green trace in Figure S11b). For (**c**) and (**d**), SERIA spectra recorded during the forward-going and reverse-going traces are shown in blue and red, respectively.

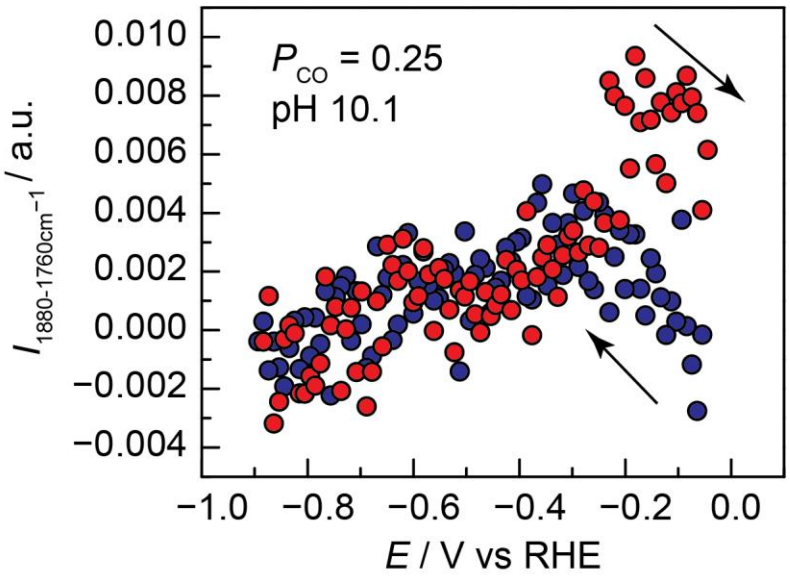

Figure S12. Potential dependence of the integrated band intensity for the IR peak spanning 1880 to 1760 cm^{-1} observed in SEIRA spectra recorded during CV scans at 2 mV s^{-1} in 0.75-atm Ar-saturated 0.1 M carbonate buffer, pH 10.1, with P_{CO} = 0.25 atm (CV shown in Figure S11b, green, and full SEIRA spectra shown in Figure S11d). Data corresponding to the forward-going and reverse-going traces are shown in blue and red, respectively.

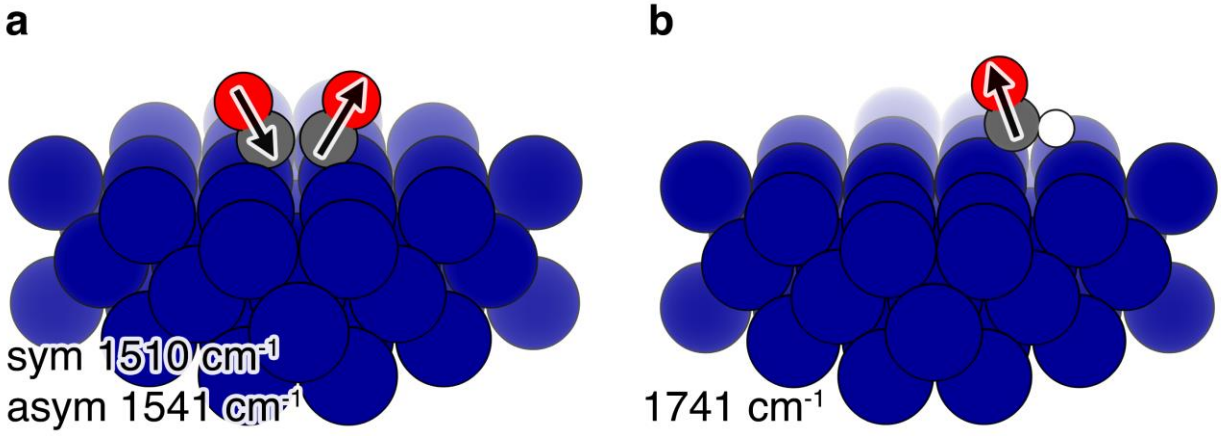

Figure S13. Calculated dominant C–O stretching vectors for surface-bound OCCO (**a**) and CHO (**b**) on Cu(100).

CHO (cm^{-1})	**OCCO (cm^{-1})**
1741	1541
1622	1510
1186	567
481	392
308	344
179	323
84	244
75	239
39	174
	118
	103
	73

Table S1. Calculated vibrational modes of surface-bound CHO and OCCO on Cu(100) surfaces from previously published[9] structures.

References

(1) Wuttig, A.; Surendranath, Y. Impurity Ion Complexation Enhances Carbon Dioxide Reduction Catalysis. *ACS Catal.* **2015**, *5*, 4479–4484.

(2) Osawa, M. Surface-Enhanced Infrared Absorption. In *Near-Field Optics and Surface Plasmon Polaritons. Topics in Applied Physics*; Kawata, S., Ed.; Springer: Berlin, 2001; Vol. 81, pp 163–187.

(3) Osawa, M. Surface Enhanced Infrared Absorption Spectroscopy. In *Handbook of Vibrational Spectroscopy*; Chalmers, J. M., Griffiths, P. R., Eds.; Wiley-VCH: Chichester, UK, 2002; pp 785–800.

(4) Osawa, M. In-Situ Surface-Enhanced Infrared Spectroscopy of the Electrode/Solution Interface. In *Diffraction and Spectroscopic Methods in Electrochemistry (Advances in Electrochemical Science and Engineering)*; Alkire, R. C., Kolb, D. M., Lipkowski, J., Ross, P. N., Eds.; Wiley-VCH: New York, 2006; pp 269–314, Vol. 9.

(5) Ataka, K.; Yotsuyanagi, T.; Osawa, M. Potential-Dependent Reorientation of Water Molecules at an Electrode/Electrolyte Interface Studied by Surface-Enhanced Infrared Absorption Spectroscopy. *J. Phys. Chem.* **1996**, *100*, 10664–10672.

(6) Osawa, M. Dynamic Processes in Electrochemical Reactions Studied by Surface-Enhanced Infrared Absorption Spectroscopy(SEIRAS). *Bull. Chem. Soc. Jpn.* **1997**, *70*, 2861–2880.

(7) Osawa, M.; Ataka, K.; Yoshii, K.; Yotsuyanagi, T. Surface-Enhanced Infrared ATR Spectroscopy for in Situ Studies of Electrode/electrolyte Interfaces. *J. Electron Spectros. Relat. Phenomena* **1993**, *64-65*, 371–379.

(8) Li, C. W.; Ciston, J.; Kanan, M. W. Electroreduction of Carbon Monoxide to Liquid Fuel on Oxide-Derived Nanocrystalline Copper. *Nature* **2014**, *508*, 504–507.

(9) Goodpaster, J. D.; Bell, A. T.; Head-Gordon, M. Identification of Possible Pathways for C–C Bond Formation during Electrochemical Reduction of CO2: New Theoretical Insights from an Improved Electrochemical Model. *J. Phys. Chem. Lett.* **2016**, *7*, 1471–1477.

(10) Perdew, J. P.; Ruzsinszky, A.; Csonka, G. I.; Vydrov, O. A.; Scuseria, G. E.; Constantin, L. A.; Zhou, X.; Burke, K. Generalized Gradient Approximation for Solids and Their Surfaces. *Phys. Rev. Lett.* **2008**, *100*, 136406.